Primary CNS lymphoma in Immunocompetent patients: Appearances on Conventional and Advanced Imaging with Review of literature

Anagha Joshi[1], Sneha Deshpande[1], Madhura Bayaskar[1*]

1. Department of radiodiagnosis, Lokmanya Tilak Municipal Medical College and General hospital, Sion, Mumbai, India

* **Correspondence:** Dr. Madhura Bayaskar, Department of radiodiagnosis, Lokmanya Tilak Municipal Medical College and General hospital Sion, Mumbai, India
(*madhura29.mb@gmail.com*)

Radiology Case. 2022 Jul; 16(7):1-17 :: DOI: 10.3941/jrcr.v16i7.4562

ABSTRACT

Primary central nervous system lymphoma (PCNSL) constitutes about 3% of all primary brain tumors and nearly 1 to 3% of all Non Hodgkin Lymphomas. In the recent years the incidence of primary CNS lymphoma is increasing in immunocompetent patients. As PCNSL are chemosensitive as well as radiosensitive, its early and accurate diagnosis is imperative for optimal management. Contrast enhanced Magnetic Resonance Imaging (MRI) is the recommended imaging modality for PCNSL; however, contrast enhanced Computed Tomography (CE-CT) is done in cases where MRI is contraindicated. Advanced imaging techniques like DWI (diffusion weighted imaging), MRS (MR Spectroscopy), MR perfusion, DTI (Diffusion tensor imaging) are important in diagnosis and help in its differentiation from other tumors.

CASE SERIES

CASE SERIES

Introduction:

CNS lymphoma constitutes two major subtypes, the most common type being secondary CNS involvement by systemic lymphoma, while the rarer variety being the primary CNS lymphoma (PCNSL) which is restricted to brain, leptomeninges, spinal cord or eyes, without involvement outside CNS at primary diagnosis [1–4].

PCNSL constitutes about 3% of all primary brain tumors and nearly 1 to 3% of all Non Hodgkin Lymphomas [3]. Majority of the PCNSL are diffuse large B cell lymphomas (95%) whereas T-cell, Burkitt, lymphoblastic, and marginal zone lymphomas constitute the rest 5% [3] . In the recent years the incidence of primary CNS lymphoma is increasing in immunocompetent patients with majority of PCNSL reported from India being in immunocompetent individuals, however the etiology of PCNSL in immunocompetent individual is still uncertain and is a mystery [1,4]. The usual age of occurrence of PCNSL is between the sixth and seventh decade but in immunocompromised patients the age of onset is earlier, that is, the fourth decade [4].

As PCNSL are chemosensitive as well as radiosensitive, its early and accurate diagnosis is imperative for optimal management [2,3]. Contrast enhanced Magnetic Resonance Imaging (MRI) is the recommended imaging modality for PCNSL; however, contrast enhanced Computed Tomography (CE-CT) is done in cases where MRI is contraindicated.

[18F]-fluorodeoxyglucose (FDG) positron emission tomography (PET) has selected utility in cerebral lymphoma, especially in diagnosis, however it is emerging as an important tool in the patients with renal dysfunction in whom the contrast is contraindicated and is also superior in determining the sensitivity of PCNSL to chemotherapy faster than MRI. FDG PET can be used in diagnosing and defining the extent of disease and some particularly smaller lesions seen on MRI may not be apparent on FDG PET and vice a versa some lesions seen on PET may initially be overlooked or misinterpreted on standard MRI [5–7].

Corticosteroids can significantly alter the imaging findings as they can shrink or vanish the tumor masking the imaging findings and confound the biopsy results, hence imaging of tumor and its biopsy should be performed before administration of steroids. Screening of the chest, abdomen and pelvis should also be performed to rule out secondary lymphoma [2–4].

Our case series reviews the typical and atypical imaging features of PCNSL in immunocompetent patients on conventional as well as advanced imaging techniques.

Review:

We retrospectively reviewed demographic, clinical and imaging features of seven consecutive patients diagnosed with PCNSL [Table 1 and Table 2], who were referred to our department for imaging over a period of one year. Of these 7 patients, four patients had undergone contrast enhanced MRI study and three patients had undergone contrast enhanced Computed Tomography (CE-CT).

MRI was done on Philips Achieva 3T machine. The MRI protocol in our institution included-fast spin echo T1WI (TR-500ms and TE-8ms), T2WI (TR-3000ms and TE-80 ms), FLAIR (TR-11000ms and TE 125ms), DWI (0,100 and 1000s/m^2), T2 FFE sequences. MR perfusion was performed followed by 3D post contrast T1 weighted spin echo sequence with slice thickness of 1mm. Multivoxel MR Spectroscopy was performed at intermediate TE (TE-135ms). DTI was performed with at least 6 diffusion encoding directions. Contrast enhanced Computed Tomography (CE-CT) were performed in three patients with acquisition of 5 mm axial section and reconstruction of 1 mm section in all three orthogonal planes.

Acquired images were evaluated for number and location of the lesions, signal intensity on conventional MR images, presence of cystic changes, calcification, hemorrhage, enhancement characteristics, peritumoral edema and mass effect if any. The MR perfusion maps were evaluated for relative cerebral blood volume (rCBV), relative cerebral blood flow (rCBF) and Time Intensity curve. The metabolite profile was studied on MR spectroscopy. DTI was studied for the pattern of involvement of the adjacent white matter tracts, if any.

Demography: Total of 7 patients were studied with mean age of 48.8 years (SD: ± 17.7 years, range- 23-72 years). Out of these, all 7 were male patients (100%).

Clinical details: The commonest clinical presentations were altered sensorium (2/7, 28.5%) and focal neurological deficits (2/7, 28.5%). The other clinical features were headache (1/7, 14.2 %), convulsions (1/7, 14.2 %) and imbalance (1/7, 14.2 %) in one patient each.

Imaging: Contrast enhanced MRI brain was performed in four patients while CECT brain was performed in three patients due to presence of contraindications to MRI.

Location and number: Seven patients exhibited a total of 24 lesions. Three patients had a solitary lesion while four patients had multiple lesions (ten lesions seen in one patient, seven lesions seen in one patient, and 2 lesions in two patients each). The lesions were supratentorial in location in five patients (5/7, 71.4%), supratentorial as well as infratentorial in one patient (1/7,14.2%) and only infratentorial in one patient (1/7, 14.2 %). Majority of the lesions (22 lesions) were supratentorial in location (22/24, 91.66%), most commonly being periventricular in location (9/22 lesions, 40.90%) with 3 of these (3/9, 33.33%) showing involvement of corpus callosum (Figure 1, 9), followed by intraventricular location (7/22, 31.8%) (Figure 7). The butterfly pattern of involvement or lesion crossing the midline involving the genu or splenium of corpus callosum was seen in two patients (2/7, 28.6%) (Figure 1A, 9). Involvement of deep grey nuclei was seen in two (28.5%) of our patients (Figure 6). One of the patients in our series, showed multiple lesions [10] with 7 of them being intraventricular in location and rest [3] being periventricular in location (Figure 7). Two lesions in infratentorial location showed involvement of cerebellar hemisphere and vermis (Figure 2). Perivenular enhancement was seen in two patients (2/7, 28.5%) (Figure 2A), subependymal enhancement was noted in one patient (1/7, 14.2%) (Figure 7) and leptomeningeal enhancement was seen in one patient (1/7, 14.2%) (Figure 2).

Size of the lesion – we considered the maximum and the minimum dimension of the largest lesion of each patient evaluated on CT and MRI. The maximum dimension of the largest lesion evaluated on computed tomography was 4 cm and the maximum dimension of the largest lesion evaluated on MRI was 5.6 cm. The minimum dimension of the largest lesion evaluated on CT was 10mm and the minimum dimension of the largest lesion evaluated on MRI was 1.5 cm. Thus the mean size of the lesion was 3.5 cm and the median was 3 cm.

Imaging appearance on CT: A total of 13 lesions were evaluated on CT. All 13 (13/13, 100%) lesions were hyperdense on non-contrast study. Three lesions showed homogenous post contrast enhancement (3/13, 23.1%) while heterogeneous enhancement was noted in 10 lesions (10/13, 76.9%).

Imaging features on Conventional MRI sequences: A total of 11 lesions were evaluated on MRI. All (11/11, 100%) lesions were isointense to hypointense on T1 WI. One of the lesions showed multiple hyperintense foci within which was corresponding to hemorrhagic foci (Figure 5B). All (11/11, 100%) lesions were hypointense on T2W and FLAIR sequences.

DWI (Diffusion weighted imaging): All (11/11, 100%) lesions showed restricted diffusion with corresponding low ADC (apparent diffusion coefficient) values (Figure 1B, Figure 5D, Figure 6E).

T2 FFE: Areas of blooming were seen in one lesion (1/11, 9 %) which corresponded to the T1 hyperintense hemorrhagic areas (Figure 5C).

Post contrast enhancement of the focal lesions: Intense homogenous enhancement was seen in ten lesions (10/11, 90.9%) (Figure 1D, Figure 6 G-J) and mild heterogenous enhancement in one lesion (1/11,9.1%) (Figure 5F).

MR Perfusion: MR Perfusion revealed marked reduction in rCBV (relative cerebral blood volume) and rCBF (relative cerebral blood flow) suggestive of lesions being hypoperfused (Figure 3B).

MR spectroscopy: MR spectroscopy revealed elevated Choline with reduced NAA and Cr levels, elevated Cho/NAA and Cho/Cr ratios in all evaluated lesions. Lipid peaks were noted in studies done in two patients (2/4, 50%) (Figure 3A).

DTI (Diffusion tensor imaging): DTI was performed in one patient which revealed decreased FA (fractional anisotropy) and ADC values and a pattern of infiltration and destruction of the corticospinal tracts and infiltration of splenium of corpus callosum and sagittal stratum in primary lesion. The mean FA value was 0.37±0.05 (Figure 4).

Leptomeningeal enhancement: Leptomeningeal enhancement was seen along inferior cerebellar foliae in one patient (1/7 patients, 14.29%)(Figure 2C).

Subependymal enhancement: Subependymal enhancement was seen in one patient (1/7 patients, 14.29%) along occipital horn of the lateral ventricle (Figure 7B,C,D).

Hemorrhage: was seen in one lesion (1/24, 4.17%) (Figure 5).

Calcification: was seen in one lesion (1/24, 4.17%) (Figure 8A).

Perilesional/ vasogenic edema on CT and MRI: Mild perilesional edema was seen in 17 lesions (17/24, 70.8%) (Figure 1). No edema was seen associated with lesions which were intraventricular in location (7/24, 21.2%) (Figure 7).

DISCUSSION

Etiology & Demographics:

We studied demographic, clinical and CT and MRI findings of 7 histologically proven cases of PCNSL in immunocompetent patients [Table 1, 2, 3]. The mean age of diagnosis in our case series was 48.8 years (SD: ± 17.7 years, range- 23-72 years) which is earlier as compared to other studies in which usual age of onset is between sixth and the seventh decade in immunocompetent patients [4,8]. Male predominance was noted in our case series which is consistent with the previous studies done by Neelakantan et al. [4] and Mansour et al. [2] with a male : female ratio of approx 1.2 to 1.7 [9].

Congenital or acquired immunosuppression is a major risk factor for PCNSL. Initially EBV infection was speculated to play a role in induction of PCNSL, however recently there is increase in the incidence of sporadic non EBV associated PCNSL in immunocompetent patient with no reported familial cases [10].

In the recent years the incidence of primary CNS lymphoma is increasing in immunocompetent patients whereas the its incidence is decreasing in HIV population due to introduction of HAART [1,4].

Clinical & Imaging Findings:

The clinical features of PCNSL include headache and/or nausea and vomiting due to raised intracranial pressure, cognitive decline or personality changes, confusion or focal neurological deficits [2,11]. In our series, the commonest clinical presentations were altered sensorium and focal neurological deficits. The other clinical features were headache, convulsions and imbalance in one patient each.

PCNSL typically presents as a solitary parenchymal mass involving the supratentorial brain parenchyma with periventricular predilection [2,8,12]. Multiplicity is also a reported feature of PCNSL [2,4,9]. Multiple lesions have been reported in 20-40% of non-AIDS PCNSL with highest reported number of lesions being eight [12–14]. In our series, multiple parenchymal lesions (4/7 cases) were more commonly seen as compared to solitary parenchymal lesion (3/7 cases), with the maximum number of lesions being ten. Majority of the lesions (22 lesions, 91.66%) in our series were supratentorial in location with involvement of the periventricular white matter and corpus callosum. We also noted multiple intraventricular lesions in one patient which is a rare, but reported pattern of involvement in PCNSL [2,15]. Infratentorial lesions in our study involved the cerebellar hemispheres and vermis.

The characteristic imaging features of PCNSL are generally attributed to various factors like hypercellularity, high nuclear cytoplasmic ratio and disruption of the blood brain barrier. On CT the lesions appear as well defined hyperdense homogenously enhancing lesions [1,2]. The same was observed in our patients with all the lesions being hyperdense on non-contrast enhanced CT. In our series, however, the lesions more commonly showed intense heterogeneous enhancement which was seen in ten lesions (10/13, 76.9%) on CECT rather than homogenous post contrast enhancement which was seen in three lesions (3/13, 23%). On pre-contrast MRI, PCNSL appears hypo- or iso-intense on T1WI, and hypo intense on T2WI and FLAIR images, with similar pattern seen in our series [1,2,4]. DWI measures diffusion of water molecules in biologic tissue and is surrogate marker of the cellularity of tissue [1,16]. Diffusion is restricted in CNS lymphoma as they are highly cellular tumors and appear hyperintense on DWI with reduced ADC values [16,17]. All the lesions in our series showed restricted diffusion with low ADC values. The ADC

measurement of the tumor is predictive of the clinical outcome and can be used as a biomarker to monitor response to the treatment with increasing ADC values suggestive of favorable prognosis [2]. Diffusion restriction can also be seen with acute ischemic stroke, the central necrosis of brain abscesses, the solid portion of high-grade gliomas, and some metastases. However, PCNSL lesions often have more restricted diffusion and lower ADC values than high-grade gliomas and metastases [1,2,16].

All the patients evaluated on post gadolinium MRI showed intense homogenous enhancement, which is in concordance with previously described reports [1,2,8,9]. Linear enhancement along perivascular spaces is highly suggestive of PCNSL [15,18]. Ring like enhancement has been reported in immunocompromised patients but is rare in immunocompetent patients. Lesions with gyral like and radial enhancement pattern, open ring enhancement have also been described [11]. Perivascular/ perivenular spread was seen in two patients (2/7, 28.5%) in our study. Leptomeningeal enhancement has been described in PCNSL [4,9], which was seen in one patient in our study, along cerebellar foliae. Subependymal enhancement has also been described in PCNSL [4,8,9] was also seen in one of our patients along one of the lateral ventricles.

Spectroscopy helps in non-invasive assessment of the biochemical environment of the tissue [1]. Lesions in our cases showed increased choline and decreased NAA, high Cho/Cr and Cho/NAA ratios with lipid peak in 50% of the cases evaluated. This has also been seen in other studies as well [1,2,4,9]. An increase in the lipid peak in absence of necrosis is considered a most specific finding in PCNSL [3]. These findings can be seen in GBM and metastases also and may not be helpful in differentiation between them and PCNSL but may help to differentiate PCNSL from other lesions [1]. Higher Glu (glutamate)/Cr, Glu/Glu+Gln (glutamine) and Cho/Cr ratios have been reported in PCNSL than GBM [3].

Perfusion studies help to demonstrate increased microvascular permeability of the lesion. It helps to assess the tumor vascularity/neovascularisation. Post processing of the data enables to calculate various physiologic parameters like rCBV, rCBF, MTT (mean transit time), TTP (time to peak). PCNSL demonstrates low rCBV and are hypoperfused as seen in our cases. The characteristic time intensity curve shown by lymphoma can be attributed to the massive leakage of contrast into the interstitial space [1,11]. Also the maximum rCBV measured in tumor tissue is typically lower in lymphomas than in other brain tumors and can help in differentiating glioblastomas and metastases from other PCNSL [2]. Enhancement–Perfusion mismatch is seen in lymphoma in DSC perfusion, low mean rCBV in an enhancing portion of the tumor is strongly suggestive of lymphoma and helps in differentiating PCNSL from other enhancing malignant lesions [19].

DTI requires measurement of the diffusion values in at least six different directions and is sensitive in detecting alterations in white matter tract integrity. Decreased FA values are seen in most brain tumors. Decreased FA and ADC values are noted in PCNSL which was also seen in our patient with pattern of infiltration and destruction of the corticospinal tracts in primary lesion with mean FA value of 0.37±0.05 [1]. Infiltration of the fibers splenium of corpus callosum and sagittal stratum on right side was also seen. PCNSL has significantly decreased FA values as compared to glioblastoma multiforme and thus may help in differentiation of these tumors [20]. However according to the recent study by Ahmed Razek et al.[21], the FA values of PCNSL were significantly greater than glioblastoma.

Another feature which is commonly associated with PCNSL is the presence of only mild perilesional edema which is less prominent than gliomas and metastases. Marked perilesional edema is uncommon probably due to the infiltrative nature of the tumor [2,4,9]. Vasogenic edema was seen adjacent to 17 lesions (17/24, 70.8%) in our study.

Hemorrhage and calcification within PCNSL lesions are rare and very few cases with these atypical features have been described [2,4,22]. In our series also, hemorrhage and calcification were present in one lesion each. These rare and atypical findings thus can be used as a useful feature to distinguish PCNSL from other tumors with calcification and hemorrhage as common feature [9]. Mansour et al. [2] in their study of CNS lymphomas in immunocompetent patients observed hemorrhage in 2 of the 36 lesions, which were hyperintense on T1 and found no calcification in any of the lesions. Hemorrhage and calcification can be seen in PCNSL after the patient receives radiation therapy or antineoplastic drugs [4]. None of the patients in our study had intratumoral or peritumoral cyst. Only one case of PCNSL presenting as cyst with mural nodule has been described with cyst related to an adjacent epidermoid cyst [4]. Insignificant number of cystic changes and hemorrhage within tumor were also observed by Ali Fazeli et al. [22] and Zhang et al [9] in their studies.

Treatment & Prognosis:

Patients with primary CNS lymphoma have extremely poor prognosis with average survival period of approximately 3.3 months in immunocompetent patients since diagnosis. Use of chemotherapy and radiation therapy can increase the mean survival period. Early diagnosis with PET or SPECT can prolong the survival period as ^{18}F-FDG PET and PET/CT showed considerable accuracy in identifying PCNSL in immunocompetent patients and can become an important radiological diagnostic tool for PCNSL [5].

Favorable prognosis can be seen in patients with age less than 60 years, those with normal or mildly impaired neurologic function and in patients with tumor confined to cerebral hemispheres or cerebellum [23].

Surgical resection of these neoplasm have no effect on survival. As patients of PCNSL have dismal prognosis recurrences have been rare in them. [10] (Table 3).

Differential Diagnosis:

Glioblastoma Multiforme

One of the important differential diagnosis/mimicker for PCNSL is glioblastoma multiforme which can be differentiated from PCNSL with the help of advanced imaging as discussed.

GBM are predominantly supratentorial in location with involvement of cerebral hemispheres and surrounding vasogenic edema [24].

The most significant MRI difference between PCNSL and GBM can be assessed on post contrast study as the enhancement pattern is more homogenous in PCNSL and heterogenous with central necrotic area in high grade glioma. Involvement of the optic tracts and basal ganglia is more commonly seen in PCNSL whereas cortical involvement is more common with high grade glioma. Another sequence which plays a pivotal role in distinguishing between the two is the DWI sequence with more restricted diffusion and lower ADC values seen in PCNSL due to its high cellularity and nuclear cytoplasmic ratio in comparison to GBM. Even though GBM have solid portion which can show diffusion restriction but their cystic-necrotic component shows high diffusion of water molecules. Relative minimum ADC has been stated to be the most accurate parameter to distinguish between PCNSL and GBM with cut off value of 0.722 and sensitivity and specificity of 74.5% and 74.1% respectively [3,24–26]. Dynamic contrast enhanced MRI can be used to distinguish the two pathologies by assessing the perfusion parameters as higher rCBV than normal tissue is seen in PCNSL but lower rCBV when compared to the GBMs. An increase in the lipid peak in absence of necrosis, higher Glu/Cr and Glu/Glu+Gln ratios have been reported in PCNSL than GBM [3]. Amide proton transfer weighted studies (APTW), which detects endogenous mobile proteins and peptides in tissue is another technique which helps in distinguishing PCNSL from GBM as homogenous hyperintensities in enhancing areas are seen in PCNSL whereas heterogenous APTW hyperintensities are seen in GBM [3,27]. With further research of application of artificial intelligence in distinguishing the two, MR image based texture analysis may be a promising tool as it describes a variety of image analysis techniques that quantify the variation in surface intensity or patterns including some which are imperceptible to the human vision [28,29].

Metastasis

Metastasis is typically located at grey-white matter interface in cerebral hemispheres followed by cerebellum and basal ganglia. Metastasis can be solitary (40%) or multiple (60%) with central necrosis , peripheral enhancement and extensive surrounding edema [3]. On DWI, metastasis shows reduced diffusivity in the peripheral enhancing area and increased diffusivity in the central necrotic area and in surrounding edema whereas PCNSL shows homogenous reduced diffusivity because of high cellularity. rCBV values are lower in PCNSL than in metastasis due to lack of neovascularity [30].

Tumefactive Demyelination (TDL)

These are usually solitary lesions, greater than 2 cm and typically involve supratentorial parenchyma centered in cerebral white matter and may extend to involve the cortical grey matter and are T2- FLAIR hyperintense with little mass effect and edema and variable enhancement patterns like homogenous , heterogeneous , open ring, closed ring , punctate, nodular and linear [3,31]

Advanced imaging features like ADC can help in noninvasive diagnosis as tumefactive demyelination lesions are mostly hypocellular with ADC values higher than the PCNSL whereas PCNSL shows homogenous low ADC values. PCNSL have higher rCBV values than tumefactive demyelination [31].

Infectious and granulomatous diseases

Toxoplasmosis encephalitis is an important differential diagnosis in patients with AIDS (Acquired Immunodeficiency Syndrome). Toxoplasmosis is commonly located at basal ganglia and at junction of the grey white matter interface and less commonly in brainstem with extensive surrounding vasogenic edema. They appear T1 iso or hypointense and T2 hyperintense during liquefactive necrosis and T2 hypointense in the post treatment period and shows nodular or ring enhancement. On DWI, toxoplasma lesions have higher ADC values than PCNSL [30]. On MRS lipid lactate peak without elevated cho/cr ratio is seen in toxoplasma encepahlitis. rCBV values are higher in PCNSL than in toxoplasma encephalitis [30] (Table 4).

Neurosarcoidosis can mimic PCNSL. MRI findings in neurosarcoidosis include leptomeningeal enhancement and multiple white matter enhancing lesions. Other investigations like serum ACE levels, CSF examination , HRCT chest and bronchoalveolar lavage can help in diagnosis of neurosarcoidosis [30].

The limitations of our case series include small sample size which can affect all the parameters of the study and few patients undergoing CT while MRI being done in other patients. Considering the higher sensitivity of MRI as compared to CT there is possibility of few lesions being missed on CT. Our study also reported the case of PCNSL in younger patient but the etiology of PCNSL in such a young age group in immunocompetent individual remains unexplained as discussed above.

TEACHING POINT

The incidence of Primary CNS Lymphoma in immunocompetent patients is increasing. Early diagnosis significantly impacts the management and prognosis as these are chemosensitive and radiosensitive tumors. Primary CNS Lymphoma commonly presents as solitary or multiple supratentorial lesions with most common locations being periventricular white matter, corpus callosum and basal ganglia, however, can be seen in atypical locations. They appear hyperdense on unenhanced CT with homogeneous or heterogeneous contrast enhancement on Contrast enhanced CT. They appear iso –hypointense on T1WI, hypointense on T2WI and show homogenous post gadolinium enhancement. Although hemorrhage and calcification are rare findings they can still be encountered in immunocompetent patients. Advanced imaging techniques like Diffusion Weighted Imaging, Magnetic resonance spectroscopy, MR perfusion, Diffusion Tensor Imaging are important in diagnosis and help in its differentiation from other tumors.

REFERENCES

1. Haldorsen IS, Espeland A, Larsson EM. Central nervous system lymphoma: Characteristic findings on traditional and advanced imaging. Am J Neuroradiol. 2011;32(6):984-92. PMID: 20616176

2. Mansour A, Qandeel M, Abdel-Razeq H, Abu Ali HA. MR imaging features of intracranial primary CNS lymphoma in immune competent patients. Cancer Imaging. 2014;14(1):1-9. PMID: 25608570

3. Chiavazza C, Pellerino A, Ferrio F, Cistaro A, Soffietti R, Rudà R. Primary CNS Lymphomas: Challenges in Diagnosis and Monitoring. Biomed Res Int. 2018;2018. PMID: 30035121

4. Sankar Neelakantan, Sunitha P Kumaran, Sanjaya Viswamitra NG. Myriad of MR imaging phenotypes of primary central nervous system lymphoma in a cohort of immunocompetent Indian patient population. ijri. 2018;28(3):296-304. PMID: 30319205

5. Zou Y, Tong J, Leng H, Jiang J, Pan M, Chen Z. Diagnostic value of using 18F-FDG PET and PET/CT in immunocompetent patients with primary central nervous system lymphoma: A systematic review and meta-analysis. Oncotarget. 2017 Jun;8(25):41518-28. PMID: 28514747

6. Ambady P, Hu LS, Politi LS, Anzalone N, Jr RFB. Primary central nervous system lymphoma?: advances in MRI and PET imaging. :1-11. Ann Lymphoma 2021;5:27. doi: 10.21037/aol-20-53

7. Krebs S, Barasch JG, Young RJ, Grommes C, Schöder H. Positron emission tomography and magnetic resonance imaging in primary central nervous system lymphoma - a narrative review. 2021;(3):1-22. PMID: 34223561

8. H. Wayne Slone, Joseph J. Blake, Rajul Shah, Sangeeta Guttikonda ECB. CT and MRI Findings of Intracranial Lymphoma. AJR. 2005;(MAY):184:1679-1685 0361-803X. PMID: 15855138

9. Zhang D, Hu L-B, Henning TD, Ravarani EM, Zou L-G, Feng X-Y, et al. MRI findings of primary CNS lymphoma in 26 immunocompetent patients. Korean J Radiol. 2010;11(3):269-77. PMID: 20461180

10. Koeller KK, Smirniotopoulos JG, Jones R V. From the Archives of the AFIP: Primary Central Nervous System Lymphoma: Radiologic-Pathologic Correlation. Radiographics. 1997;17(6):1497-526. PMID: 9397461

11. Zhang D, Hu LB, Henning TD, Ravarani EM, Zou LG, Feng XY, et al. MRI findings of primary CNS lymphoma in 26 immunocompetent patients. Korean J Radiol. 2010;11(3):269-77. PMID: 20461180

12. Mohile NA, Abrey LE. Primary central nervous system lymphoma. Neurol Clin. 2007;25(4):1193-207. PMID: 17964031

13. Küker W, Nägele T, Korfel A, Heckl S, Thiel E, Bamberg M, et al. Primary central nervous system lymphomas (PCNSL): MRI features at presentation in 100 patients. J Neurooncol. 2005 Apr;72(2):169-77. PMID: 15925998

14. Coulon A, Lafitte F, Hoang-Xuan K, Martin-Duverneuil N, Mokhtari K, Blustajn J, et al. Radiographic findings in 37 cases of primary CNS lymphoma in immunocompetent patients. Eur Radiol. 2002 Feb;12(2):329-40. PMID: 11870430

15. Go JL, Lee SC, Kim PE. Imaging of primary central nervous system lymphoma. Neurosurg Focus. 2006 Nov;21(5):E4. PMID: 17134120

16. Zacharia TT, Law M, Naidich TP, Leeds NE. Central nervous system lymphoma characterization by diffusion-weighted imaging and MR spectroscopy. J Neuroimaging. 2008 Oct;18(4):411-7. PMID: 18494774

17. Schroeder PC, Post MJD, Oschatz E, Stadler A, Bruce-Gregorios J, Thurnher MM. Analysis of the utility of diffusion-weighted MRI and apparent diffusion coefficient values in distinguishing central nervous system toxoplasmosis from lymphoma. Neuroradiology. 2006 Oct;48(10):715-20. PMID: 16947010

18. Eichler AF, Batchelor TT. Primary central nervous system lymphoma: presentation, diagnosis and staging. Neurosurg Focus. 2006 Nov;21(5):E15. PMID: 17134117

19. Goyal P, Kumar Y, Gupta N, Malhotra A, Gupta S, Gupta S, et al. Usefulness of enhancement-perfusion mismatch in differentiation of CNS lymphomas from other enhancing malignant tumors of the brain. Quant Imaging Med Surg. 2017 Oct;7(5):511-9. PMID: 29184763

20. Toh CH, Castillo M, Wong AMC, Wei KC, Wong HF, Ng SH, et al. Primary cerebral lymphoma and glioblastoma multiforme: Differences in diffusion characteristics evaluated with diffusion tensor imaging. Am J Neuroradiol. 2008;29(3):471-5. PMID: 18065516

21. Abdel Razek AAK, El-Serougy L, Abdelsalam M, Gaballa G, Talaat M. Differentiation of Primary Central Nervous System Lymphoma From Glioblastoma: Quantitative Analysis Using Arterial Spin Labeling and Diffusion Tensor Imaging. World Neurosurg [Internet]. 2019;123:e303-9. Available from: https://doi.org/10.1016/j.wneu.2018.11.155 PMID: 30502475

22. Fazeli MA, Janamiri Z, Zali A, Seddighi A, Seddighi A, Ashrafi F, et al. MRI Findings of Primary CNS Lymphoma in 20 Patients of Stereotaxic Ward. Int Clin Neurosci J [Internet]. 2016;3(3):158-63. Available from: https://journals.sbmu.ac.ir/Neuroscience/article/view/14422 https://doi.org/10.22037/icnj.v3i3.14422

23. Michalski JM, Garcia DM, Kase E, Grigsby PW, Simpson JR. Primary central nervous system lymphoma: analysis of prognostic variables and patterns of treatment failure. Radiology. 1990 Sep;176(3):855-60. PMID: 2389047

24. Malikova H, Koubska E, Weichet J, Klener J, Rulseh A, Liscak R, et al. Can morphological MRI differentiate between primary central nervous system lymphoma and glioblastoma? Cancer Imaging. 2016;16. PMID: 27894359

25. Guo AC, Cummings TJ, Dash RC, Provenzale JM. Lymphomas and high-grade astrocytomas: comparison of water diffusibility and histologic characteristics. Radiology. 2002 Jul;224(1):177-83. PMID: 12091680

26. Wen J-B, Huang W-Y, Xu W-X-Z, Wu G, Geng D-Y, Yin B. Differentiating Primary Central Nervous System Lymphomas From Glioblastomas and Inflammatory Demyelinating Pseudotumor Using Relative Minimum Apparent Diffusion Coefficients. J Comput Assist Tomogr. 2017;41(6):904-9. PMID: 28708728

27. Jiang S, Yu H, Wang X, Lu S, Li Y, Feng L, et al. Molecular MRI differentiation between primary central nervous system lymphomas and high-grade gliomas using endogenous protein-based amide proton transfer MR imaging at 3 Tesla. Eur Radiol. 2016 Jan;26(1):64-71. PMID: 25925361

28. Kunimatsu A, Kunimatsu N, Kamiya K, Watadani T, Mori H, Abe O. Comparison between glioblastoma and primary central nervous system lymphoma using MR image-based texture analysis. Magn Reson Med Sci. 2018;17(1):50-7. PMID: 28638001

29. Alcaide-Leon P, Dufort P, Geraldo AF, Alshafai L, Maralani PJ, Spears J, et al. Differentiation of enhancing glioma and primary central nervous system lymphoma by texture-based machine learning. Am J Neuroradiol. 2017;38(6):1145-50. PMID: 28450433

30. Shim WH, Kim HS, Choi C-G, Kim SJ. Comparison of Apparent Diffusion Coefficient and Intravoxel Incoherent Motion for Differentiating among Glioblastoma, Metastasis, and Lymphoma Focusing on Diffusion-Related Parameter. PLoS One. 2015;10(7):e0134761. PMID: 26225937

31. Given CA, Stevens BS, Lee C. The MRI Appearance of Tumefactive Demyelinating Lesions. Am J Roentgenol. 2004;182(1):195-9. PMID: 14684539

FIGURES

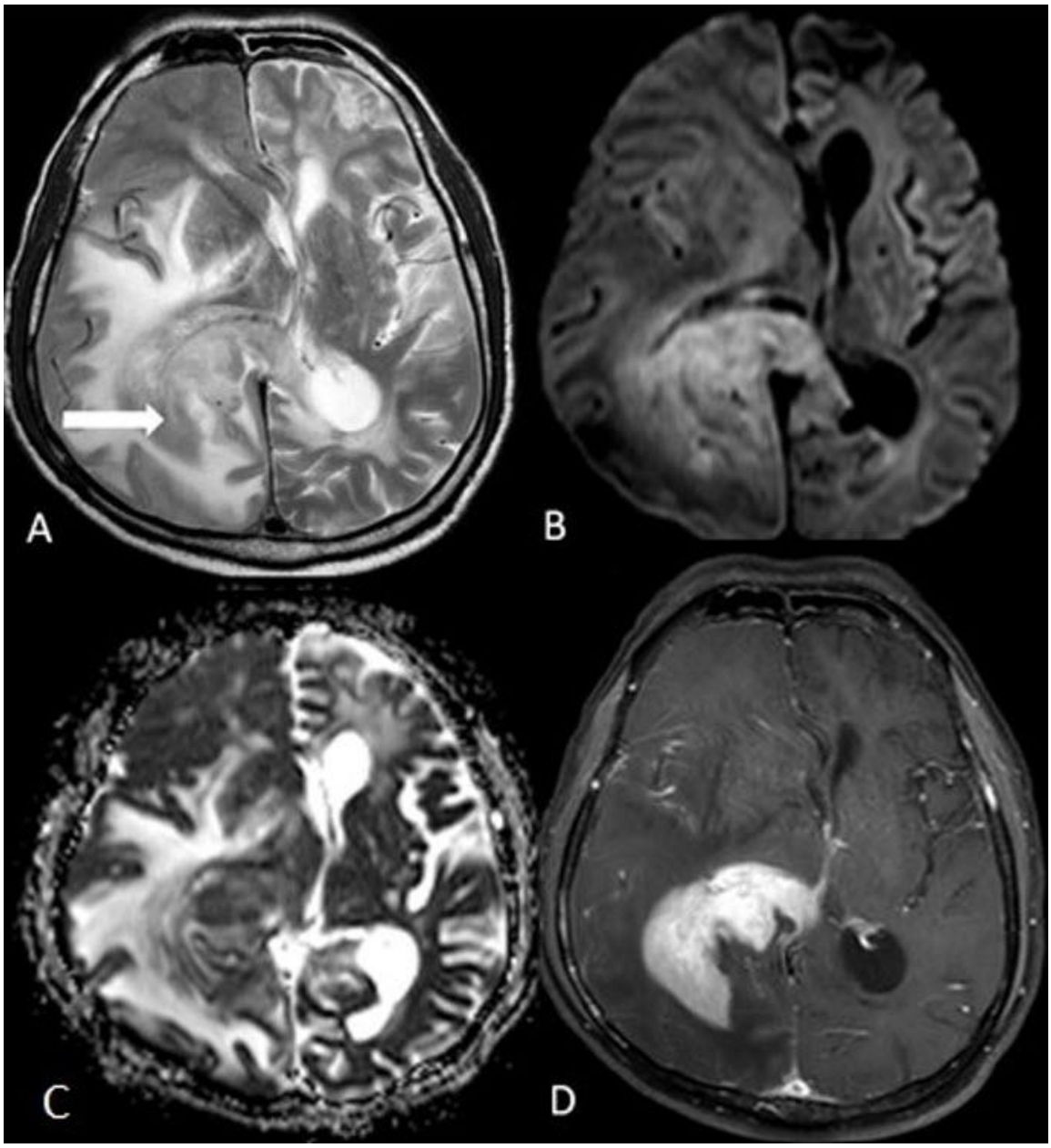

Figure 1: 60 Year old male with primary CNS lymphoma

Findings: Axial MRI images reveals a (A) T2 hypointense infiltrative lesion involving the splenium of corpus callosum and the adjacent right parieto-occipital periventricular white matter (arrow) (B) It shows restricted diffusion with (C) corresponding low ADC values with (D) intense homogenous post contrast enhancement

Technique: Philips Achieva 3T machine (A) T2WI (TR-3000ms and TE-80 ms) (B) DWI (1000s/m^2) (C) ADC (D) 3D post contrast T1 weighted spin echo sequence with slice thickness of 1mm. Contrast material - Gadovist, dose 0.1ml/kg body weight

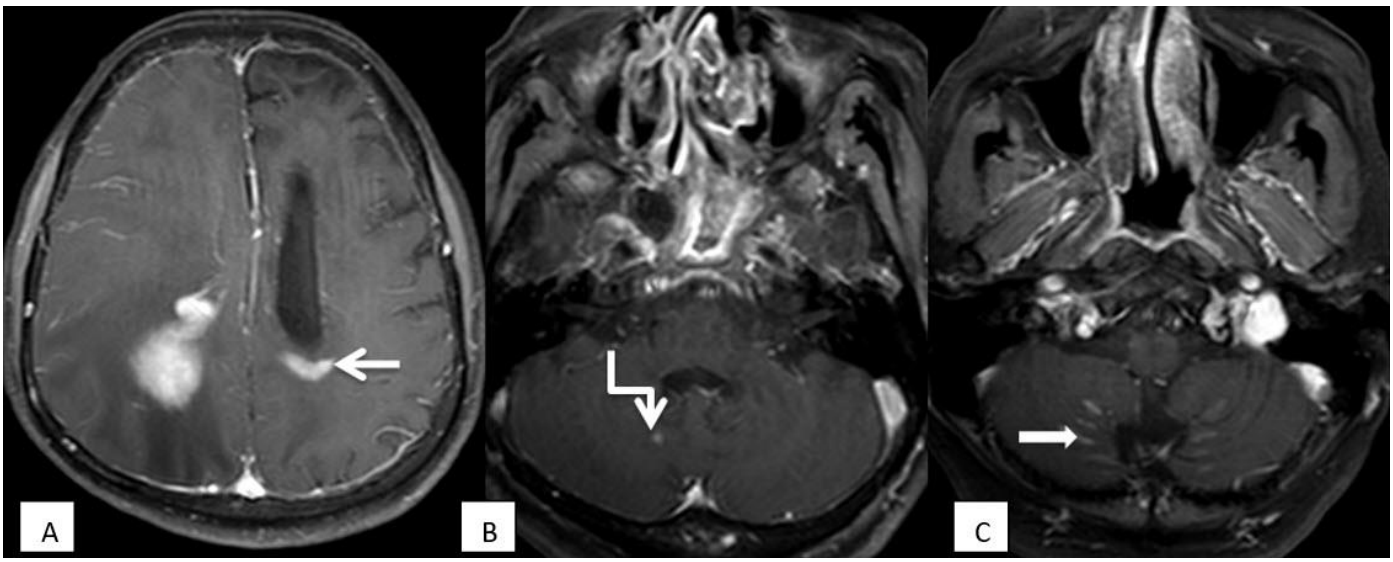

Figure 2: 60 Year old male with primary CNS lymphoma

Findings: Axial post contrast MRI images showing (A) perivenular spread posterior to the body of left lateral ventricle (arrow) (B) a small enhancing nodule in right cerebellar hemisphere adjacent to fourth ventricle (angled arrow) and (C) leptomeningeal enhancement along bilateral cerebellar folia (arrows)

Technique: Philips Achieva 3T machine 3D post contrast T1 weighted spin echo sequence with slice thickness of 1mm. Contrast material - Gadovist, dose 0.1ml/kg body weight

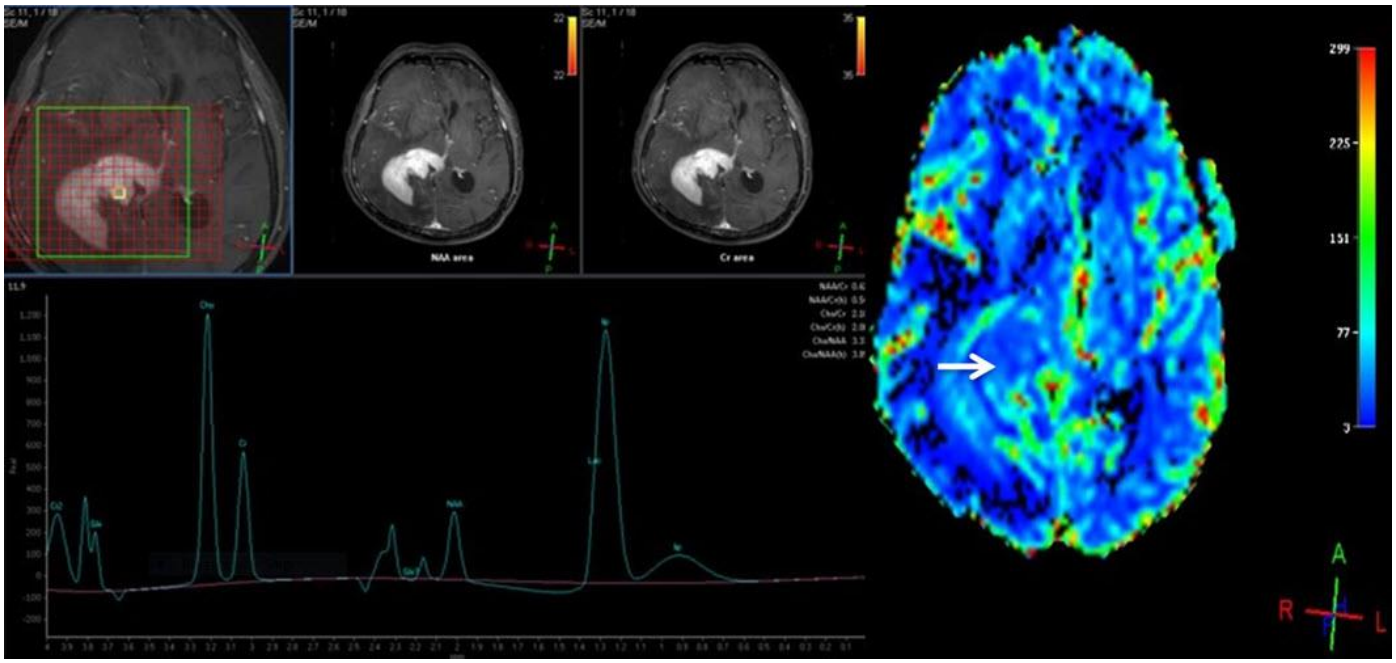

Figure 3: 60 Year old male with primary CNS lymphoma

Findings: (A) MR Spectroscopy shows elevated choline peak with reduced NAA levels and a lipid lactate peak. (B) MR perfusion shows lesion is hypoperfused with low rCBF.

Technique: Philips Achieva 3T machine (A) Multivoxel MR Spectroscopy performed at intermediate TE (TE-135ms), (B) MR Perfusion

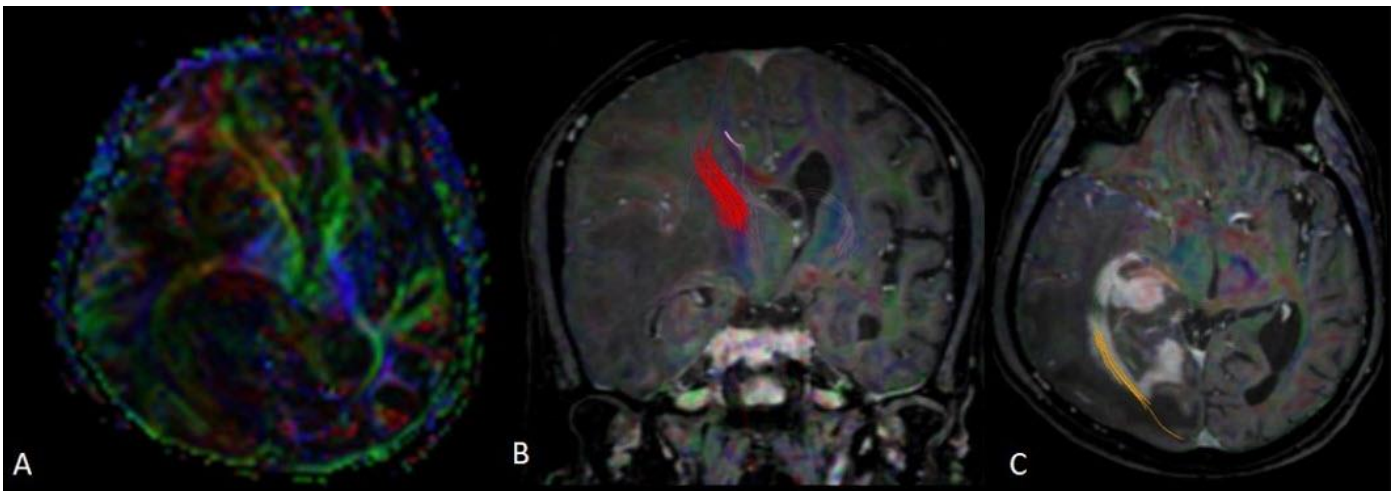

Figure 4: 60 Year old male with primary CNS lymphoma
Findings: (A) FA map shows displaced right corticospinal tracts and splenium of corpus callosum with reduced colour hue (B) shows destruction of the right corticospinal tracts seen in red (C) shows infiltration of the fibres of sagittal stratum (yellow colour) on right side.
Technique: Philips Achieva 3T machine (A) FA map, (B and C) Diffusion Tensor Imaging

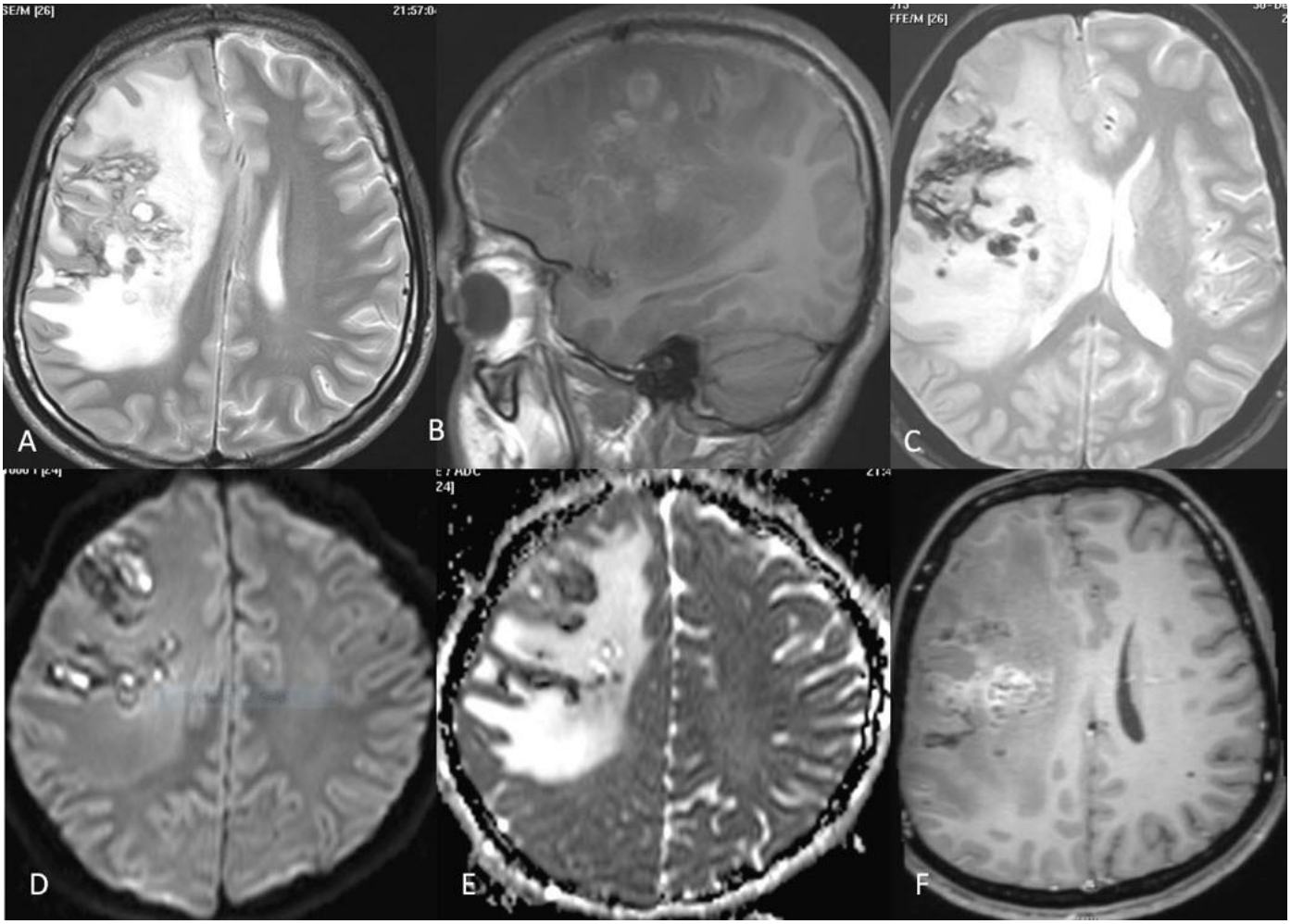

Figure 5: 23 Year old male with primary CNS lymphoma
Findings: MRI images showing a mass lesion involving the right frontal lobe appearing (A) hypointense on T2 (B) with T1 hyperintense areas within (C) showing blooming on GRE and (D) few areas of restricted diffusion with (E) corresponding low ADC values. (F) It shows patchy areas of contrast enhancement.
Technique: Philips Achieva 3T machine. (A) T2WI (TR-3000ms and TE-80 ms) (B) T1WI (TR-500ms and TE-8ms) (C) T2 FFE (D) DWI (1000s/m2) (E) ADC (F) 3Dpost contrast T1 weighted spin echo sequence with slice thickness of 1mm. Contrast material - Gadovist, dose 0.1ml/kg body weight

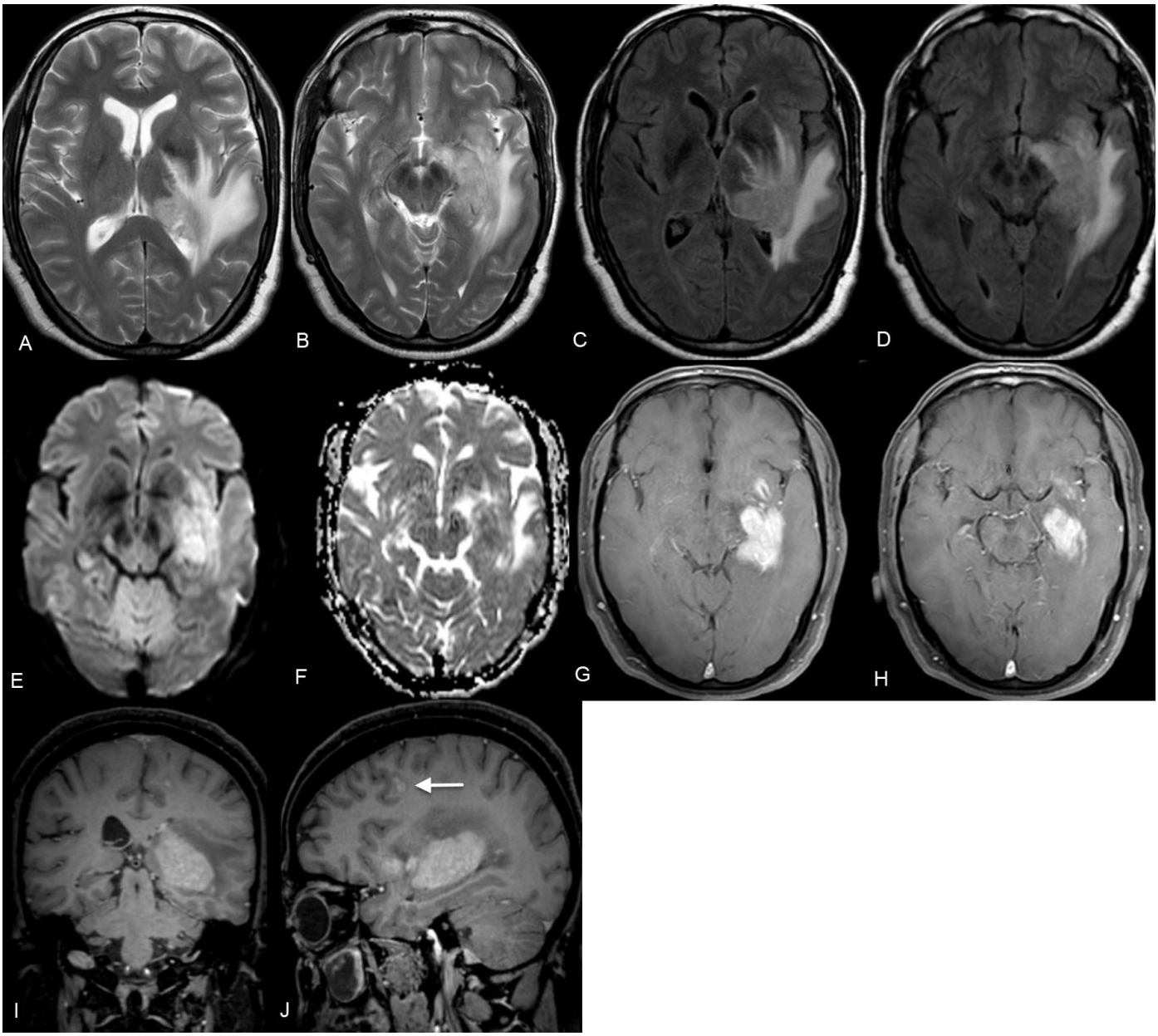

Figure 6: 45 Year old male with primary CNS lymphoma

Findings: MRI images showing a mass lesion involving the left thalamus & basal ganglia & adjacent temporal periventricular white matter appearing (A,B) hypointense on axial T2 and FLAIR (C,D) and showing (E) areas of restricted diffusion with (F) corresponding low ADC values. (G-J) It shows homogenous post contrast enhancement. A tiny enhancing satellite lesion (arrow) seen in left frontal lobe(J).

Technique: Philips Achieva 3T machine. (A,B) T2WI (TR-3000ms and TE-80 ms) (C,D) FLAIR (TR- 11000 and TE-125) (E) DWI (1000s/m^2) (F) ADC (G-J) 3Dpost contrast T1 weighted spin echo sequence with slice thickness of 1mm. Contrast material - Gadovist, dose 0.1ml/kg body weight

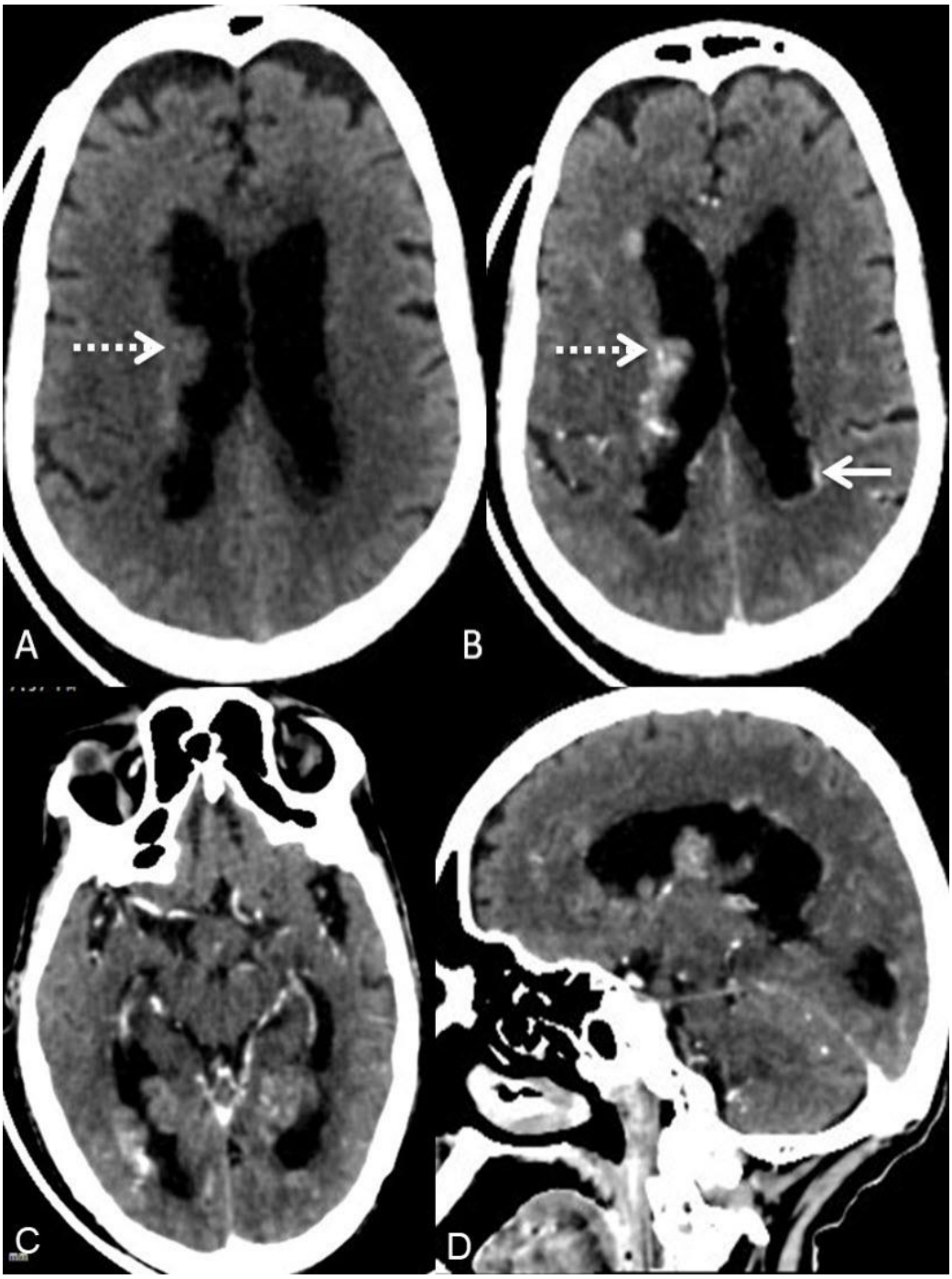

Figure 7: 72 Year old male with primary CNS lymphoma

Findings: Axial (A) non contrast and (B,C)axial (D) sagittal post contrast CT images showing well defined hyperdense subependymal and periventricular lesions along the bilateral lateral ventricles (dotted arrow) which show heterogeneous post contrast enhancement. Ependymal enhancement is also seen (solid arrow) (B).

Technique: Contrast enhanced Computed Tomography(CE-CT) performed with acquisition of 5 mm axial section and reconstruction of 1 mm section in all three orthogonal planes. Philips 64-slices MD CT scanner, 400 mAs, 120 kV, 1 mm slice thickness. Contrast material - Omnipaque 1.5ml/kg body weight

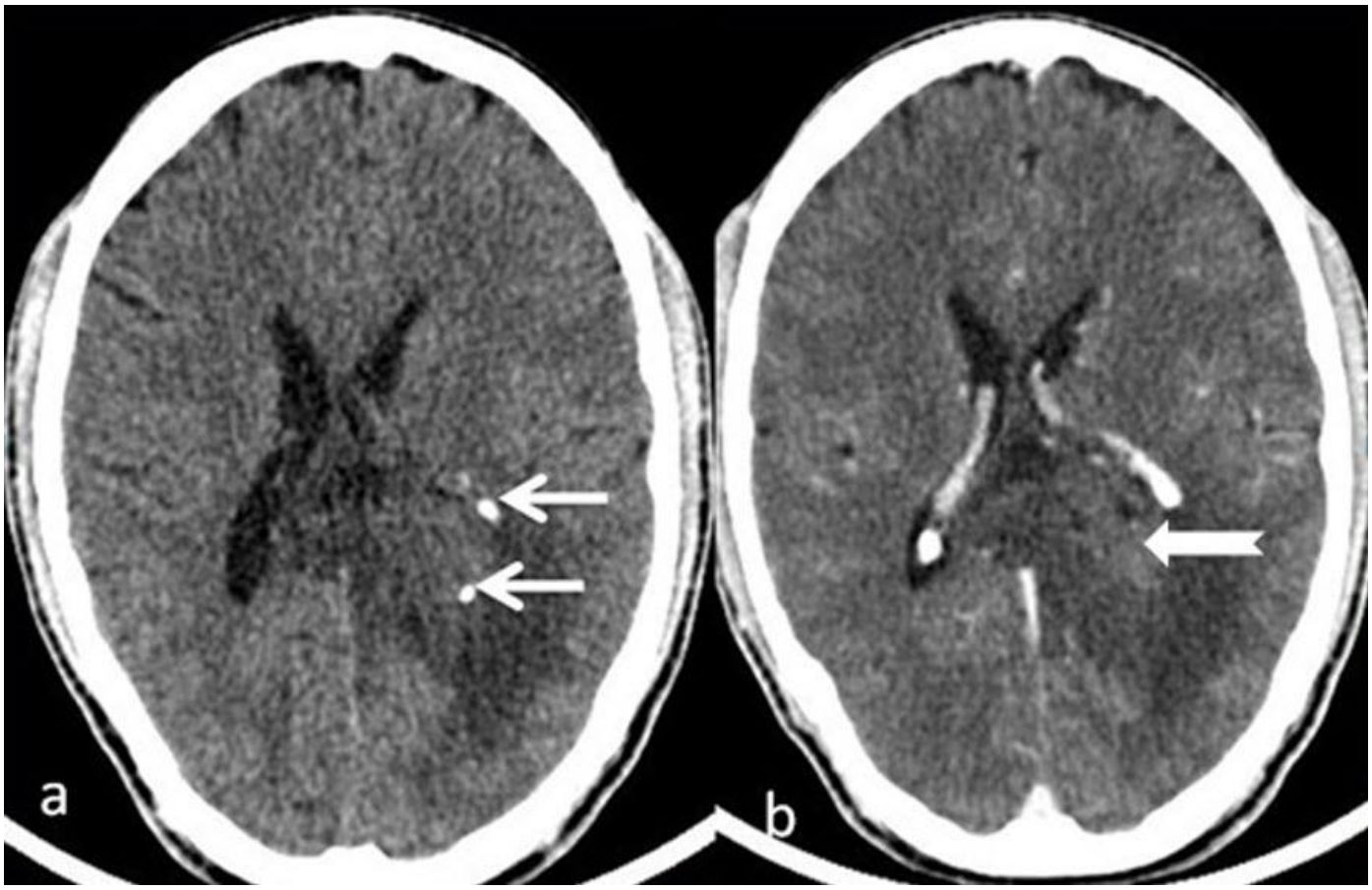

Figure 8: 40 Year old male with primary CNS lymphoma

Findings: (A) Unenhanced and (B) Post contrast axial images reveal a hypodense lesion involving the splenium of corpus callosum and adjacent left parietal periventricular white matter showing few tiny calcific foci within (arrows). It shows minimal post contrast enhancement (notched white arrow).

Technique: Philips 64-slices MD CT scanner, 400 mAs, 120 kV, 1 mm slice thickness. Contrast material - Omnipaque 1.5ml/kg body weight

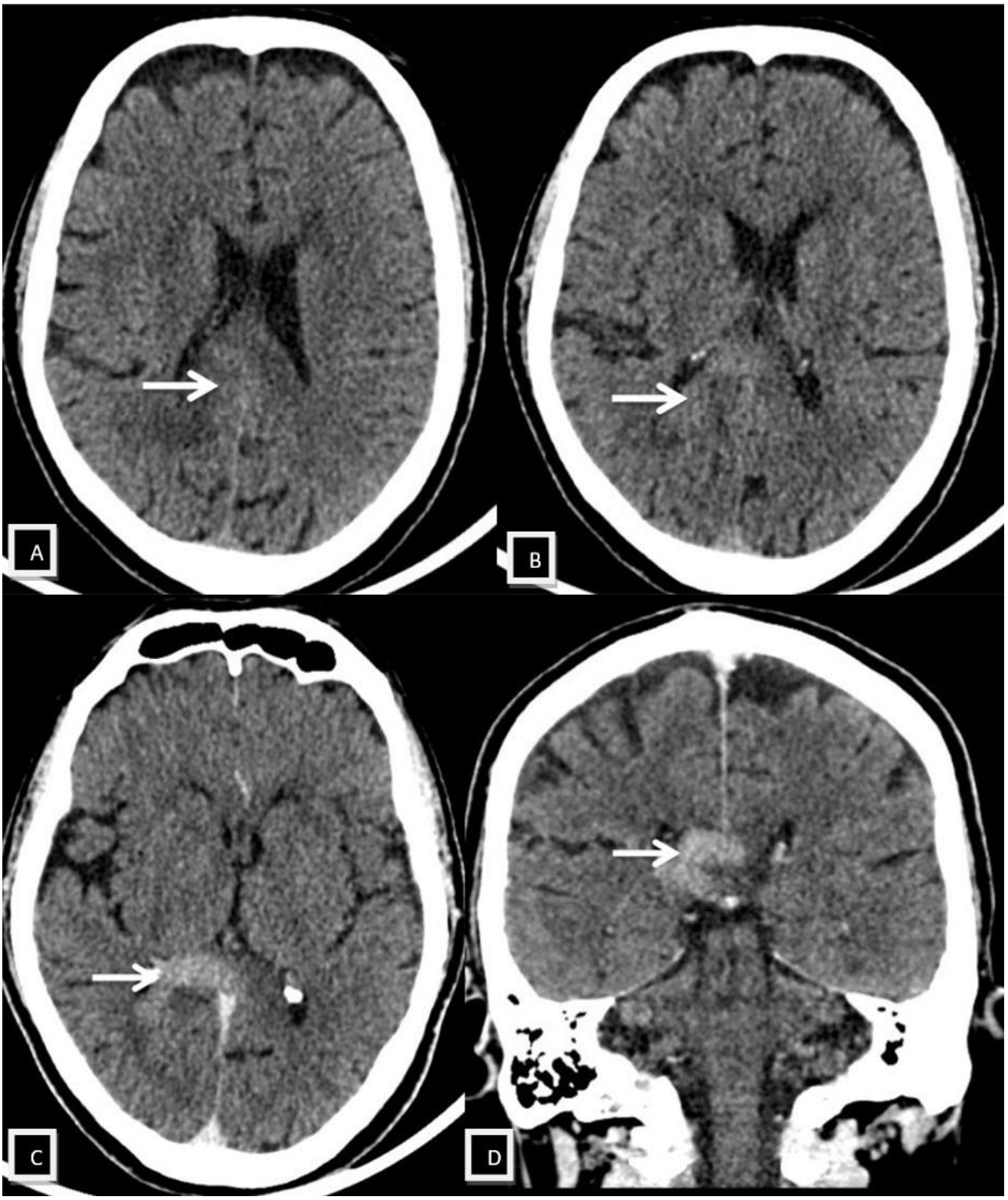

Figure 9: 66 Year old male with primary CNS lymphoma

Findings: (A, B) non contrast axial images showing an ill defined hyperdense lesion involving the splenium of corpus callosum and Post contrast axial(C) and coronal (D) images reveal a homogenous post contrast enhancement of the lesion and crossing the midline .

Technique: Philips 64-slices MD CT scanner, 400 mAs, 120 kV, 1 mm slice thickness, Contrast material - Omnipaque 1.5ml/kg body weight

	Case 1	**Case 2**	**Case 3**
Age (Years)	40	66	72
Gender	Male	Male	Male
Total number of lesions	Single	Two	Ten
Location (number of lesions at that site)	Splenium of corpus callosum & adjacent parietal periventricular white matter (1)	Basal ganglia and thalamus (1); Splenium of corpus callosum & adjacent peri-trigonal parietooccipital periventricular white matter (Butterfly lesion) (1)	Intraventricular- in bilateral lateral ventricles (7), Periventricular (3)
Plain	Hyperdense	Hyperdense	Hyperdense
Enhancement	Present	Present	Present
Calcification	Present	Absent	Absent
Hemorrhage	Absent	Absent	Absent
Meningeal /subependymal enhancement	Absent	Absent	Present

Table 1: Summary of CT findings in patients with primary CNS lymphoma in immunocompetent patients imaged at our institute.

	Case 1	**Case 2**	**Case 3**	**Case 4**
Age (Years)	60	45	23	36
Gender	Male	Male	Male	Male
Total number of lesions	2	7	1	1
Location (number of lesions at that site)	Splenium of corpus callosum & adjacent parieto-temporo-occipital periventricular white matter (Butterfly lesion) (1), right cerebellar hemisphere (1)	Thalamus & basal ganglia & adjacent temporal periventricular white matter in (1): bilateral high frontal and ipsilateral parietal white matter (6)	Frontal periventricular white matter	Cerebellar hemisphere extending to Superior and middle cerebellar peduncles
T1	Hypointense	Hypointense	Hypointense with hyperintense foci	Hypointense
T2	Hypointense	Hypointense	Hypointense	Hypointense
DWI	Restriction	Restriction	Restriction	Restriction
Enhancement	Present	Present	Present	Present
Calcification	Absent	Absent	Absent	Absent
Hemorrhage	Absent	Absent	Present	Absent
Meningeal enhancement	Present	Absent	Absent	Absent

Table 2: Summary of MRI findings in patients with primary CNS lymphoma in immunocompetent patients imaged at our institute.

Etiology	Initially EBV infection was speculated to play a role in induction of PCNSL, however recently there is increase in the incidence of sporadic non EBV associated PCNSL in immunocompetent patient with no reported familial cases.
Incidence	PCNSL constitutes about 3% of all primary brain tumors and nearly 1 to 3% of all Non-Hodgkin Lymphomas
Gender ratio	M:F- 1.3 to 1.7
Age predilection	Male predilection
Risk factors	Congenital or acquired immunosuppression is a major risk factor for PCNSL
Treatment	Chemotherapy, radiotherapy, and surgical resection
Prognosis	Patients with primary CNS lymphoma have extremely poor prognosis with average survival period of approximately 3.3 months in immunocompetent patients since diagnosis
Imaging findings	**MRI** – *T1 WI:* usually isointense to hypointense, may show hemorrhagic foci. *T2W and FLAIR:* hypointense. *DWI:* restricted diffusion with corresponding low ADC values *T2 FFE:* may rarely show areas of blooming *Post contrast enhancement* usually shows intense homogenous enhancement *MR Perfusion:* marked reduction in rCBV and rCBF suggestive of lesions being hypoperfused *MR spectroscopy:* elevated Choline with reduced NAA and Cr levels, elevated Cho/NAA and Cho/Cr ratios, can show lipid peaks *DTI:* reveals decreased FA and ADC values and a pattern of infiltration Leptomeningeal enhancement: Leptomeningeal enhancement can be seen Subependymal enhancement: can be seen Hemorrhage: rarely seen Calcification: rarely seen. Perilesional/ vasogenic edema on CT and MRI: commonly associated. **CT** – usually hyperdense on plain CT with homogenous or heterogeneous post contrast enhancement

Table 3: Summary table of Primary central nervous system lymphoma (PCNSL).

	Location	**MRI features helpful in differentiation**		
		ADC	**Enhancement pattern**	**MR Perfusion**
PCNSL	Predominantly supratentorial in location with involvement of the periventricular white matter and corpus callosum. Has surrounding vasogenic edema Involvement of the optic tracts and basal ganglia is more common	PCNSL has homogenous low ADC values	PCNSL shows intense homogenous enhancement	PCNSL has lower rCBV values
GBM	Predominantly supratentorial with involvement of cerebral hemispheres with vasogenic edema. Cortical involvement is more common with high grade glioma.	GBM have ADC values higher as compared to PCNSL	GBM exhibits heterogeneous enhancement with central necrotic area	GBM has rCBV values higher than PCNSL
METASTASIS	Grey-white matter interface in cerebral hemispheres followed by cerebellum and basal ganglia with surrounding vasogenic edema	Metastasis have reduced diffusivity in the peripheral enhancing area and increased diffusivity in the central necrotic area and in surrounding edema	Metastasis usually shows peripheral enhancement with central necrotic area	Metastases have rCBV values higher than PCNSL
TDL	Usually solitary lesions, greater than 2 cm and typically involve supratentorial parenchyma centered in cerebral white matter and may extend to involve the cortical grey matter.	TDL lesions are mostly hypocellular with ADC values higher than the PCNSL	TDL usually exhibit variable enhancement patterns like homogenous, heterogeneous , open ring, closed ring , punctate, nodular and linear.	Tumefactive demyelination has lower rCBV values than PCNSL
TOXOPLASMA	commonly located at basal ganglia and at junction of the grey-white matter interface and less commonly in brainstem with extensive surrounding vasogenic edema	Toxoplasma lesions have higher ADC values than PCNSL	Toxoplasma lesions show ring or nodular enhancement pattern.	Toxoplasma lesions have rCBV values lower than PCNSL

Table 4: Differential diagnosis table for Primary central nervous system lymphoma (PCNSL).

ABBREVIATIONS

AIDS - Acquired Immunodeficiency Syndrome
Cho - Choline
Cr - Creatine
DTI - Diffusion tensor imaging
DWI - Diffusion weighted imaging
CE -CT - Contrast enhanced Computed Tomography
GBM - Glioblastoma multiforme
HAART - Highly active antiretroviral therapy
MTT - Mean transit time
MRI - Magnetic Resonance Imaging
MRS - Magnetic resonance spectroscopy
NAA - N - acetyl aspartate
PCNSL - Primary central nervous system lymphoma
rCBF - Relative cerebral blood flow
rCBV - Relative cerebral blood volume
TDL - Tumefactive demyelination
TTP - Time to peak

KEYWORDS

Primary CNS lymphoma; immunocompetent; magnetic resonance imaging; computed tomography; advanced imaging techniques